

Influence of equation of state on interpretation of electrical conductivity measurements in strongly coupled tungsten plasma

S I Tkachenko, P R Levashov, and K V Khishchenko

Institute for High Energy Densities, Joint Institute for High Temperatures,
Russian Academy of Sciences, Izhorskaya 13/19, Moscow 125412, Russia

E-mail: svt@ihed.ras.ru

Abstract. We study the influence of equation-of-state (EOS) model on the interpretation of electrical conductivity measurements in strongly coupled plasma of tungsten by Korobenko *et al.* (2002 *Plasma Physics Reports* **28**(12) 1008–1016). Three different semiempirical EOS models for tungsten are used. Discrepancies in obtained thermodynamic parameters and specific resistivity values as compared with calculation results of Korobenko *et al.* are analysed.

PACS numbers: 64.30.+t, 72.15.Cz, 52.25.-b

1. Introduction

Electrical explosion of wires or foils is an effective way to study thermophysical properties of matter in a wide range of densities and temperatures [1, 2]. This is one of a few methods, which allows one to obtain both thermodynamic properties and kinetic coefficients in the same experiment. For example, electrical resistance can be calculated from experimental time dependencies of the heating current and voltage. To determine specific properties it should be known also the cross-section area of the conductor as a function of time. As geometric sizes of the sample may be not measured in the process of expansion it is reasonable to use the results of numerical simulation. In this case calculated properties of matter are determined, in particular, by an equation-of-state (EOS) model. In the present work we study the influence of the EOS model to the values of electrical conductivity of strongly coupled tungsten plasma based on data from Korobenko *et al.* [3].

2. Description of experiment

The experiments on electrical conductivity measurements [3] were carried out in a plane geometry. A tungsten foil stripe with the length $l_z = 10$ mm, width $h = 1.5$ mm and thickness $2a = 20$ μm was placed between two glass plates with the thickness $a_1 = 5$ mm. Side slits were shielded with thin mica stripes. In the experiment under consideration the skin layer thickness δ is significantly larger than the foil thickness. Cartesian coordinate system is introduced as follows: x -axis is perpendicular to the foil plate, y -axis is directed along the smaller side of the foil, and z -axis — along the

bigger side. In 1D process the foil expands along the x -axis, the magnetic induction B is directed along the y -axis, and the heating current I as well as the electric field intensity E are directed along the z -axis.

The foil was heated by the impulse of current; the time dependencies of the current through the sample $I(t)$ and voltage drop $U(t)$ were registered (figure 1). Then it was calculated the resistive part of the voltage drop $U_R(t)$, electrical resistance $R(t) = U_R(t)I^{-1}(t)$ and Joule heat $q(t)$. Other values required for conductivity calculation can be obtained by means of numerical simulation. Assuming that the current density j is distributed uniformly over the cross-section of the foil and depends only on time, i.e. $j(t) = I(t)S^{-1}(t)$, where $S(t) = 2a(t)h$, from the Maxwell equation $j(t) = \mu^{-1}\partial B/\partial x$ (SI system of units is used, μ is the magnetic permeability) one can calculate $B(t, x) = \mu I(t)xS^{-1}(t)$. So it is possible to determine the x - t -dependencies of foil parameters as a numerical solution of only a set of hydrodynamic equations with the Ampere force $jB = \mu I^2(t)xS^{-2}(t)$ and energy input $jE = U(t)I(t)V^{-1}(t)$, where $V(t) = S(t)l_z$ is the foil volume.

The results of calculation by such a technique not allowing for magnetic field diffusion were presented in work [3].

3. Modeling

Assuming that spatial perturbations of the sample form are small and electron and ion temperatures are equal each other, the set of 1D magnetohydrodynamic (MHD) equations in Lagrangian description for the foil heating can be represented as follows:

$$dm/dt = 0, \quad (1)$$

$$\rho dv/dt = -\partial P/\partial x - (2\mu)^{-1}\partial B^2/\partial x, \quad (2)$$

$$\rho d\varepsilon/dt = -P\partial v/\partial x + \partial(\kappa\partial T/\partial x)/\partial x + j^2/\sigma, \quad (3)$$

$$d(\mu B)/dt = \partial(\sigma^{-1}\partial B/\partial x)/\partial x, \quad (4)$$

where m is the mass, v is the particle velocity, ρ is the density, T is the temperature, P is the pressure, ε is the specific internal energy, σ is the electrical conductivity, κ is the thermal conductivity. Initial conditions for the set of equations (1)–(4) are written as follows: $\rho(x, 0) = \rho_0$, $v(x, 0) = 0$, $T(x, 0) = T_0$, $B(x, 0) = 0$. The conditions on the symmetry plane $x = 0$ and on the surface $x = a(t)$ of the foil, as well as on the outer boundary of the glass plate $x = a_1$ are as follows: $v(0, t) = 0$, $v(a, t) = da/dt$, $v(a_1, t) = 0$, $B(0, t) = 0$, $B(a, t) = \mu I(t)/2h$, $\partial T/\partial x|_{x=0} = 0$, $\partial T/\partial x|_{x=a-0} = \partial T/\partial x|_{x=a+0}$, $T(a_1, t) = T_0$, $\partial P/\partial x|_{x=0} = 0$, $P(a-0, t) = P(a+0, t)$, $P(a_1, t) = P_0$. Here ρ_0 , T_0 , and P_0 correspond to normal conditions.

We used three different EOS models for tungsten [4–6]. Semiempirical multi-phase EOS [4] in a form of functions $P = P(\rho, T)$ and $\varepsilon = \varepsilon(\rho, T)$ (EOS1) takes into account the effects of high-temperature melting, evaporation, and ionization. This EOS agrees with the collection of experimental data on static and shock compression as well as on adiabatic and isobaric expansion of the metal, see details in [4]. Caloric EOS [5] in a functional form $P = P(\rho, \varepsilon)$ (EOS2) neglects phase transitions; however it describes available shock-wave experiments within a good accuracy. The soft-sphere EOS [6] as functions $P = P(\rho, T)$ and $\varepsilon = \varepsilon(\rho, T)$ with coefficients from [7] (EOS3) considers evaporation of metal and has been calibrated using isobaric expansion experiments

but does not take into account melting and gives understated density at normal temperature and pressure.

As EOS1 allows for more effects and agrees with wider collection of data including the region of parameters of the considered experiment [3] this model is assumed to be more reliable than EOS2 and EOS3. However that may be, the correct EOS can be chosen (not necessarily amongst three used models) only in the case of direct thermodynamic measurements in the range of interest.

To describe the properties of glass we used caloric EOS $P = P(\rho, \varepsilon)$ [8].

The conductivity of tungsten was determined by the relation

$$\sigma = I(t)l_z U^{-1}(t)S^{-1}(t) \quad (5)$$

using the experimental dependencies $I(t)$ and $U(t)$ [3] except for the stage of heating up to $T = 10$ kK. In case of EOS1 at low temperatures we used the semiempirical formulas [9–11] for the electrical conductivity $\sigma = \sigma(\rho, T)$ taking into account melting effect instead of experimental functions because of noise on the measured time dependence of voltage at the initial stage. The thermal conductivity in case of EOS1 was calculated according to the Wiedemann–Franz law, $\kappa = k_{WF}T\sigma$, where k_{WF} is the Wiedemann–Franz constant. In cases of EOS2 and EOS3 during the initial stage we used time dependence of voltage $U(t)$ obtained in numerical modeling with EOS1. Thus in these cases the electrical conductivity was determined according to (5) during the whole heating process. The thermal conductivity effects in cases of EOS2 and EOS3 were neglected.

4. Results

We carried out a number of simulations of the experiment using 1D MHD model as described in the previous section. In figure 2 shown are time dependencies of the specific internal energy $\varepsilon(t)$ resulting from numerical modeling with three above-mentioned EOS. One can see that all three curves $\varepsilon(t)$ are very close during the initial heating stage.

The calculated pressure at the symmetry plane and at the foil surface depending on the specific internal energy at the same layers is shown in figure 3 in comparison with results from simulations of Korobenko *et al.* [3]. It can be seen that the melting process leads to oscillations of pressure $P(\varepsilon)$ near the symmetry plane of the foil (see curve at $x = 0$ for EOS1 in figure 3). If melting is neglected (like in calculations with EOS2 and EOS3 models) the pressure dependencies $P(\varepsilon)$ are smooth. The dynamics of the process is to some extent determined by the EOS model: after the melting EOS1 gives the fastest pressure rise during expansion, EOS2 — the slowest one. At the later stage of the heating EOS1 and EOS2 result in close pressure values while EOS3 shows 15% lower pressures.

The EOS model used in work [3] for the interpretation of experimental data is based upon the soft-sphere EOS [6] and takes into account ionization effects according to the mean atom model [12]. This EOS is unpublished and this fact complicates the qualitative analysis of distinctions. Nevertheless, figure 3 shows that the calculated pressure [3] in the process of foil heating is always lower than in present work; the same situation is observed for temperature. The simulation with EOS3 gives the closest result to that of the work [3]; this coincidence can be explained by similar EOS models used in these calculations.

One can see in figure 3 that parameters in the foil are distributed homogeneously except for the moment of melting which is clearly distinguishable by pressure oscillations. After melting thermodynamic states of the foil though sometimes very close to the binodal are always in liquid or supercritical plasma state (figure 4). However, inhomogeneity in temperature distribution appears at the late stage of the expansion process. For example according to modeling with EOS1 the scale of this inhomogeneity can be distinctly seen in figure 4 where the thermodynamic tracks of different layers of the foil are shown. Distinctions in the methodology of simulation and description of thermodynamic properties of tungsten lead to systematically higher values of electrical resistivity in our interpretation (maximum excess is about 60% for simulation with EOS1) than after Korobenko *et al.* [3] (figure 5).

It is worth to mention that during the heating process the measured voltage begins to drop at time $t \sim 750$ ns and soon (at $t \sim 850$ ns) current begins to rise (see figure 1). This effect in work [3] is connected with the beginning of transition into “dielectric” (plasma) state. Actually there is a drop in resistance at the later stage of the experiment [3], however there is no noticeable change in specific resistance (see figure 5, $\varepsilon > 10$ kJ/g). From figure 4 it can be seen that supercritical (plasma) state of tungsten, $\rho \leq \rho_{cr}$, is reached at temperature $T \sim 20$ kK, which corresponds to time $t \sim 0.6$ μ s and specific internal energy $\varepsilon \sim 5$ kJ/g. It is known that the character of electrical conductivity changes from metal-like to plasma-like near the critical density [13], $\rho_{cr} = 4.854$ g/cm³ for tungsten according to EOS1, so one can expect that the resistivity dependence should change its behavior at values of internal energy $\varepsilon \sim 5$ kJ/g. As this is not the case in figure 5 we offer an alternative explanation of the “saturation” of electrical conductivity. Namely we assume that a breakdown of interelectrode gap takes place along the glass surface at $t \sim 750$ ns (the density and specific internal energy of tungsten foil at this moment are $\rho \sim 2$ g/cm³ and $\varepsilon \sim 8$ kJ/g).

We tried to reproduce the experimental time dependence of voltage using time dependence of current as input data together with wide-range conductivity models for tungsten [13, 14] and EOS1 model. The results of simulation with the conductivity model [13] are shown in figure 1. We could well describe the voltage data up to $t \sim 500$ ns and satisfactory up to $t \sim 750$ ns, but when the voltage began to drop in the experiment it continued to rise in our calculations. It is possible to reproduce the maximum around $t \sim 750$ ns on the experimental voltage dependence only by use of a breakdown model in the simulation. Assuming that the breakdown occurs on the boundary between the glass plate and tungsten foil we increased the electrical conductivity value in region $0.95 \leq x/a(t) \leq 1$ by an order of magnitude linearly during time interval from $t = 750$ to 900 ns. It can be easily seen in figure 1 that in this case we have much better agreement with experimental time dependence of voltage. Simulations with electrical conductivity model [14] showed much more worse results than that with the model [13] and are not displayed in figure 1.

Thus either a breakdown occurs during the expansion of the foil or one can formulate an electrical conductivity model, which will be able to reproduce the voltage maximum. To solve this dilemma is an aim of a future work.

5. Conclusions

In this work we have analyzed the experiment on electrical conductivity measurements of strongly coupled tungsten plasma under heating by the current pulse. We have used

1D MHD simulation and different EOS models to study distribution of parameters in the foil. We have also tried to reproduce experimental voltage time dependence using two electrical conductivity models.

We can conclude that pressure, density and temperature are distributed almost homogeneously across the foil except for the melting stage of the process. The dynamics of the heating and expansion is determined by the EOS model giving rise to distinctions in electrical resistivity values up to 60%.

Moreover, the last stage of the experiment is probably influenced by the shunting breakdown of the interelectrode gap. These facts indicate that even in the case of the foil heating regime [3], where certain efforts have been taken for achievement of homogeneous distribution of thermophysical parameters to simplify interpretation, there are still open problems to treat experimental data. We believe that further investigations of thermodynamic and transport properties of tungsten plasma will be helpful for the creation of adequate wide-range EOS and electrical conductivity models.

Acknowledgements

The authors are grateful to V. N. Korobenko, A. D. Rakhel, and A. I. Savvatimskiy for valuable comments. Thanks are also owed to V. I. Oreshkin and E. M. Apfelbaum for providing with tungsten electrical conductivity tables.

This work was done under financial support of the Russian Foundation for Basic Research, Grants No. 04-02-17292, 05-02-16845, and 05-02-17533.

References

- [1] Lebedev S V and Savvatimskiy A I 1984 *Sov. Phys. Uspekhi* **27**(10) 749–771
- [2] Gathers G R 1986 *Rep. Progr. Phys.* **49**(4) 341–396
- [3] Korobenko V N, Rakhel A D, and Savvatimskiy A I 2002 *Plasma Phys. Rep.* **28**(12) 1008–1016
- [4] Khishchenko K V 2005 in V E Fortov *et al.*, eds, *Physics of Extreme States of Matter — 2005* (Chernogolovka: IPCP RAS) pp 170–172
- [5] Khishchenko K V 2004 *Tech. Phys. Lett.* **30**(10) 829–831
- [6] Young D A 1977 A soft-sphere model for liquid metals Tech. rep. Lawrence Livermore Laboratory Report UCRL-52352
- [7] Hess H, Kloss A, Rakhel A, and Schneidenbach H 1999 *Int. J. Thermophys.* **20**(4) 1279–1288
- [8] Khishchenko K V, Lomonosov I V, and Fortov V E 1996 in S C Schmidt and W C Tao, eds, *Shock Compression of Condensed Matter — 1995* (Woodbury, New York: AIP Press) pp 125–128
- [9] Knoepfel H 1970 *Pulsed High Magnetic Fields* (Amsterdam: North Holland)
- [10] Tkachenko S I, Khishchenko K V, Vorob'ev V S, Levashov P R, Lomonosov I V, and Fortov V E 2001 *High Temp.* **39**(5) 728–742
- [11] Tkachenko S I, Khishchenko K V, and Levashov P R 2005 *Int. J. Thermophys.* **26**(4) 1167–1179
- [12] Basko M M 1985 *High Temp.* **23**(3) 388–396
- [13] Oreshkin V I, Baksht R B, Labetskiy A Y, Rousskikh A G, Shishlov A V, Levashov P R, Khishchenko K V, and Glazyrin I V 2004 *Tech. Phys.* **49**(7) 843–848
- [14] Apfelbaum E M 2003 *High Temp.* **41**(4) 466–471

List of figures

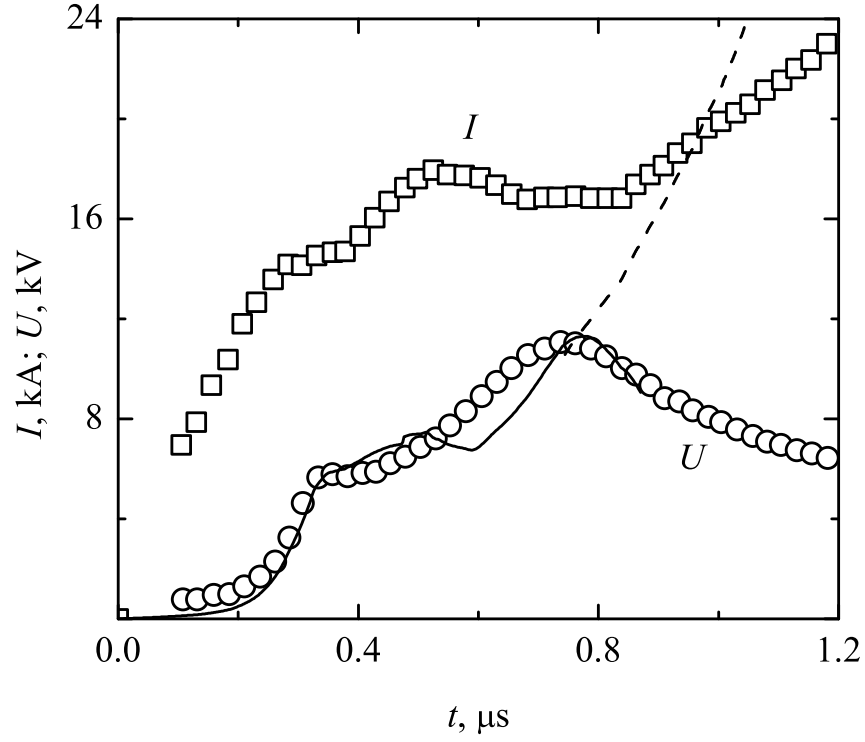


Figure 1. Current and voltage versus time: I is the current, U is the voltage, markers correspond to data from measurements of Korobenko *et al.* [3], lines denote results of numerical simulation of present work with conductivity model [13] taking into account breakdown effect (solid line) as well as disregarding breakdown (dashed line).

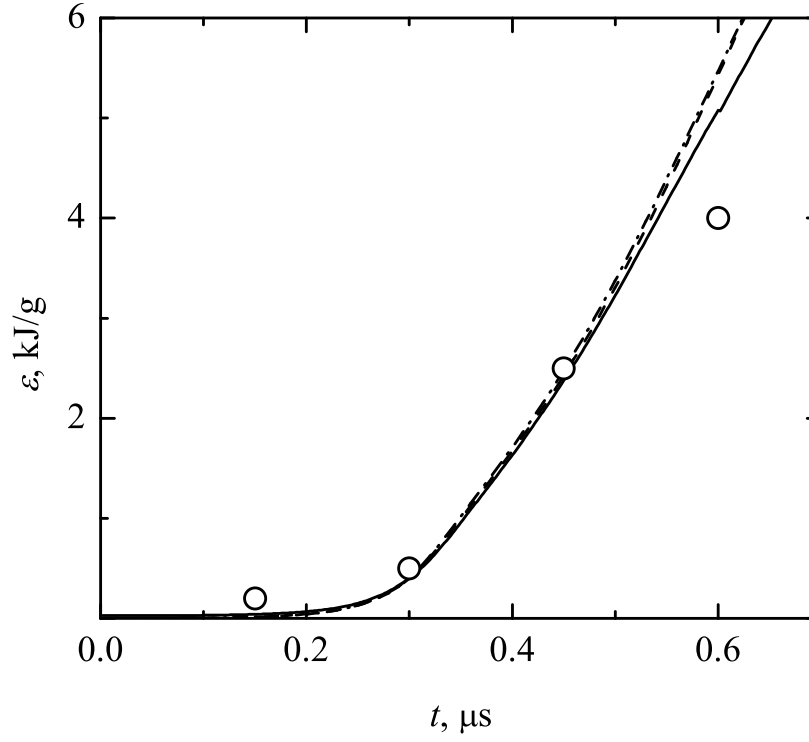


Figure 2. Specific internal energy versus time in the foil during heating calculated basing on measurements of Korobenko *et al.* [3]: circles are from simulations of Korobenko *et al.* [3], lines correspond to results of present work simulations in case of EOS1 (solid line), EOS2 (dashed line), and EOS3 (dash-dotted line).

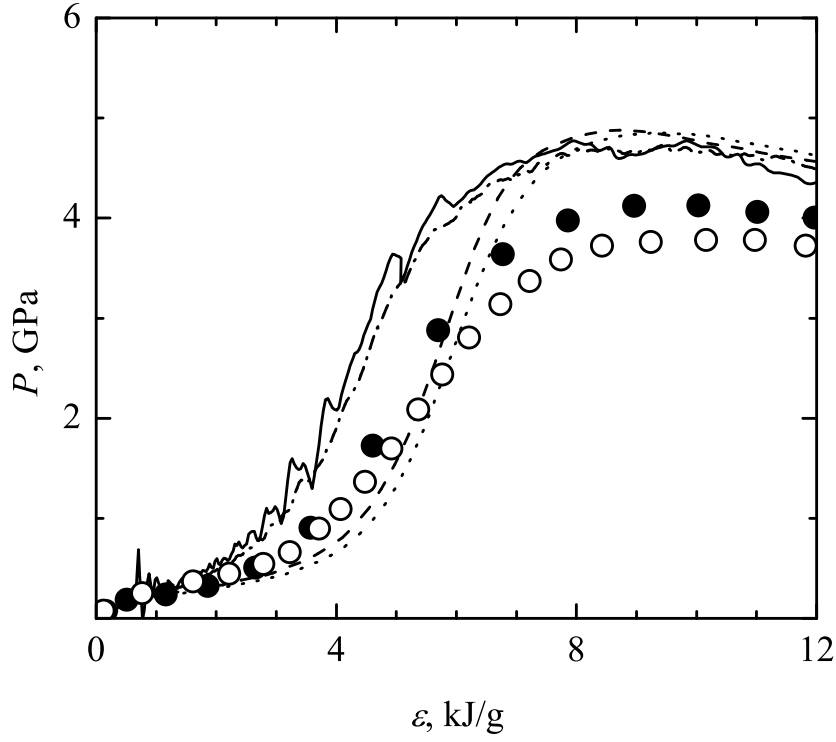


Figure 3. Pressure versus specific internal energy in the foil during heating from calculations based on measurements of Korobenko *et al.* [3]: open circles are from simulations of Korobenko *et al.* [3], lines and solid circles denote results of numerical simulations of present work in case of EOS1 (solid and dash-dotted lines, for layers $x = 0$ and $a(t)$ correspondingly), EOS2 (dashed and dotted lines, $x = 0$ and $a(t)$ correspondingly), and EOS3 (solid circles, $x = 0$).

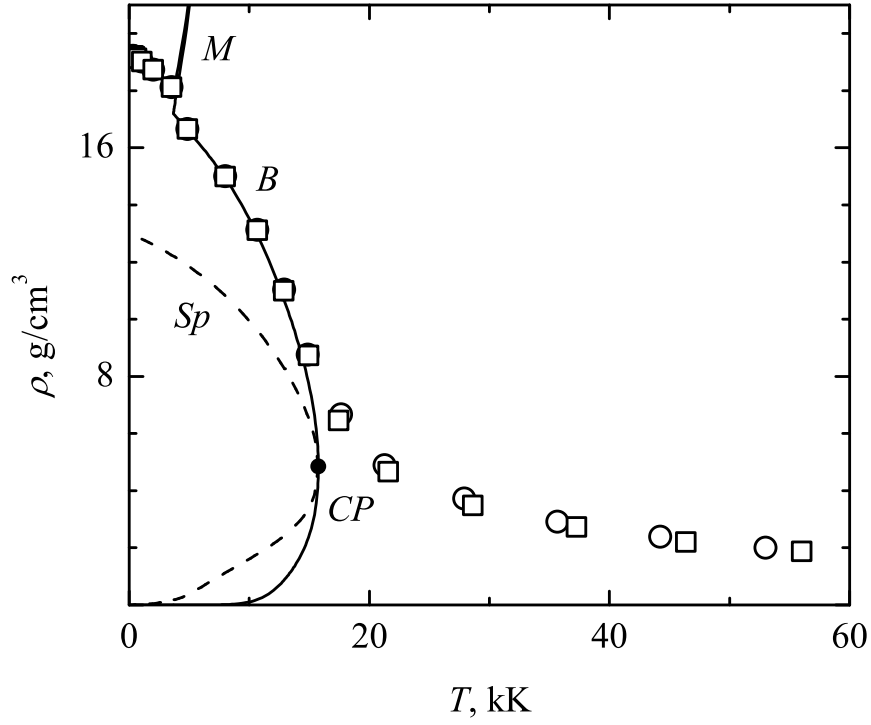


Figure 4. Phase diagram of tungsten [4] and phase trajectories: M is the melting region, B is the boundary of liquid–gas transition region, CP is the critical point, Sp are spinodals of the liquid and gas phases, circles denote states at the symmetry plane of the foil during heating, each square corresponds to state on the foil surface at the same moment as the nearest circle.

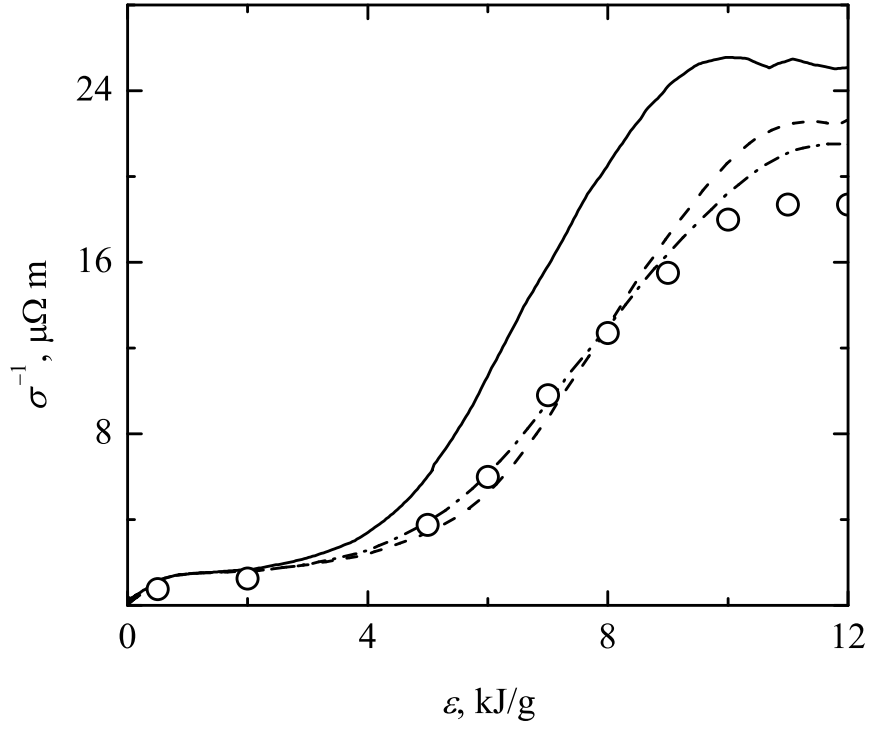


Figure 5. Specific electrical resistivity of tungsten versus specific internal energy in the foil during heating from calculations based on measurements of Korobenko *et al.* [3]: circles are from simulations of Korobenko *et al.* [3], lines correspond to results of present work simulations in case of EOS1 (solid line), EOS2 (dashed line), and EOS3 (dash-dotted line).